The antipsychotic drug pimozide is a novel chemotherapeutic agent for adult T cell leukemia

Chie Ishikawa
University of the Ryukyus: Ryukyu Daigaku
Naoki Mori (naokimori50@gmail.com)
University of the Ryukyus https://orcid.org/0000-0003-3998-6711

Research Article

Keywords: Adult T cell leukemia, Human T cell leukemia virus type 1, Pimozide, Reactive oxygen species, Signal transduction

Posted Date: March 11th, 2021

DOI: https://doi.org/10.21203/rs.3.rs-272455/v1

Abstract

Patients with adult T cell leukemia (ATL), caused by the human T cell leukemia virus type 1 (HTLV-1), exhibit poor prognosis owing to drug resistance. Pimozide, a dopamine D2 receptor subfamily antagonist and antipsychotic drug, has been shown to exhibit anticancer activity. Herein, we investigated whether pimozide exerts anti-ATL effects and explored the mechanisms underlying these effects. While pimozide inhibited cell growth and survival in HTLV-1-infected T cells, it exerted limited effects on uninfected T cells. The dopamine D2 receptor subfamily mRNA expression levels in HTLV-1-infected T cells were high. Pimozide induced G1 cell cycle arrest concomitant with the upregulation of p21/p27/p53 and the suppression of cyclin D2/E, CDK2/4/6 and c-Myc expression and pRb phosphorylation. Pimozide also induced apoptosis via the activation of caspases and upregulation of pro-apoptotic proteins and downregulation of anti-apoptotic proteins. Additionally, it promoted ROS generation and increased the expression of the ER stress marker ATF4 and the DNA damage-inducible protein GADD45a and the phosphorylation of the DNA damage marker H2AX. Furthermore, pimozide-induced cytotoxicity was partially inhibited by a ROS scavenger and pan-caspase and necroptosis inhibitors, indicating the involvement of caspase-dependent and -independent lethal pathways. The activities of the NF-κB, Akt, STAT3/5 and AP-1 signaling pathways were inhibited via the dephosphorylation of IκBα, IKKα/β, Akt and STAT3/5, in addition to reduced JunB and JunD expression in HTLV-1-infected T cells in response to pimozide treatment. Pimozide also exhibited potent anti-ATL activity in the xenograft mouse model. These findings demonstrated the efficacy of pimozide as a potential therapeutic agent for ATL.

Introduction

Adult T cell leukemia (ATL) is an intractable peripheral T cell neoplasm caused by infection with the retrovirus human T cell leukemia virus type 1 (HTLV-1) [1]. The lifetime risk of developing ATL in HTLV-1 carriers is estimated to be 6 − 7% for men and 2 − 3% for women in Japan [1]. ATL exhibits a diversity in its clinical features such as leukocytosis with increased abnormal lymphocytes, lymphadenopathy, hepatosplenomegaly, skin lesions, hypercalcemia and frequent complication of opportunistic infections [2, 3]. At present, the first-line treatment for patients with ATL comprises a combination of chemotherapy along with the administration of humanized anti-CCR4 antibodies or antiviral agents, interferon-α plus zidovudine [2]. However, patients with ATL exhibit poor prognosis owing to resistance to chemotherapy and immunosuppression [2, 3], which necessitates the designing of more effective and less toxic treatment strategies.

Drug repurposing is currently an important application in the identification of novel uses for existing drugs that are beyond the scope of the original medical indication. Since treatment options for patients with ATL are limited and systemic therapies rarely lead to durable responses, ATL may benefit more from drug repurposing. Notably, the incidence of certain cancer types has been reported to be apparently reduced in patients with schizophrenia [4]. Antipsychotics are suggested to be the potential mediators of this effect [4]. Certain antipsychotic agents have been shown to exhibit cancer-specific cytotoxic potential [5]. Pimozide, an orally active antipsychotic drug used to treat paranoid personality disorder, delusional

disorder, delusions of parasitosis, Tourette's syndrome, and resistant phonic and motor tics, has been reported to exhibit anticancer activities [6]. Pimozide inhibited cell proliferation, colony formation and sphere formation of certain types of carcinomas [6]. In the present study, we attempted to explore whether pimozide can be repurposed effectively in the treatment of ATL and investigate the potential underlying mechanism.

Materials And Methods

Cell lines and cell culture

Cells from HTLV-1-transformed T cell lines MT-2, MT-4, SLB-1 and HUT-102; ATL-derived T cell lines MT-1 and TL-Oml; and uninfected T cell lines Jurkat, CCRF-CEM and MOLT-4 were cultured in RPMI-1640 medium (Nacalai Tesque, Inc., Kyoto, Japan) supplemented with 1% penicillin/streptomycin (Nacalai Tesque, Inc.) and 10% fetal bovine serum (Biological Industries, Kibbutz Beit Haemek, Israel). The MT-2, MT-4 and MOLT-4 cells were provided by Dr. Naoki Yamamoto (Tokyo Medical and Dental University, Tokyo, Japan). The SLB-1 cells were obtained from Dr. Diane Prager (UCLA School of Medicine, Los Angeles, CA, USA). The TL-Oml and CCRF-CEM cells were obtained from Dr. Masahiro Fujii (Niigata University, Niigata, Japan). The HUT-102, MT-1 and Jurkat cells were provided by Fujisaki Cell Center, Hayashibara Biochemical Laboratories, Inc. (Okayama, Japan).

Reagents

Pimozide and z-VAD-FMK were purchased from Cayman Chemical Company (Ann Arbor, MI, USA) and Promega Corp. (Madison, WI, USA), respectively. N-acetyl-L-cysteine (NAC) and necrostatin-1 were obtained from Wako Pure Chemical Industries (Osaka, Japan) and Abcam (Cambridge, UK), respectively.

Cell growth and cytotoxicity assays

A water-soluble tetrazolium (WST)-8 assay kit (Nacalai Tesque, Inc.) was used to assess cell proliferation and toxicity. Cells were cultured in 96-well plates and treated with pimozide at different concentrations for up to 72 h. After the WST-8 reagent was added to each well and the contents were incubated, the absorbance was measured at 450 nm using a Wallac 1420 Multilabel Counter (PerkinElmer, Inc., Waltham, MA, USA). Triplicate wells were used for each culture condition. The optical density of each sample was compared to that of the control.

Cell cycle analysis

The CycleTEST Plus DNA Reagent kit (Becton-Dickinson Immunocytometry Systems, San Jose, CA, USA) was used for staining with propidium iodide (PI), which is used to label nuclear DNA. The DNA content of individual nuclei was analyzed using the Epics XL Flow Cytometer (Beckman Coulter, Inc., Brea, CA, USA) and the MultiCycle software (version 3.0; Phoenix Flow Systems, San Diego, CA, USA). Histograms of PI fluorescence intensity were produced, and the percentage of total cells at each phase of the cell cycle was determined.

Apoptosis analysis

The cells were treated with pimozide for up to 48 h, followed by permeabilization by incubation with digitonin, following which the cells were labeled with a phycoerythrin-conjugated APO2.7 antibody (1:10; Beckman Coulter, Inc., Marseille, France), as described previously [7]. The percentage of apoptotic cells was quantified immediately after staining using an Epics XL Flow Cytometer. In addition, to evaluate the morphological features of the nuclei, the cells were stained with Hoechst 33342 (Dojindo Molecular Technologies, Inc., Kumamoto, Japan) and observed under a DMI6000 microscope (Leica Microsystems, Wetzlar, Germany).

Caspase activity assay

The activity levels of caspase-3, caspase-8 and caspase-9 were quantified using Colorimetric Caspase Assay kits (Medical & Biological Laboratories, Co., Nagoya, Japan) in accordance with the manufacturer's instructions. In brief, the cells were lysed in the lysis buffer provided with the kit, and the cell lysates were incubated with the respective caspase-specific labeled substrates. The chromophore ρ-nitroanilide released upon cleavage from the substrates was quantified using a Wallac 1420 Multilabel Counter. Caspase activity was measured as the ratio between the colorimetric output in the treated sample and that in the control, with the value of the latter set to 1.

Reverse transcriptase (RT)-PCR

Total RNA was isolated from the cultured cells using the TRIzol reagent (Invitrogen Life Technologies, Carlsbad, CA, USA). Reverse transcription was performed using a PrimeScript RT-PCR kit (Takara Bio, Inc., Otsu, Japan). PCR was performed using a combination of individual sequence-specific primer sets. The following primers were used: 5'-TGTACAATACGCGCTACAGCTCCA-3' (sense) and 5'-ATGCACTCGTTCTGGTCTGCGTTA-3' (antisense) for the dopamine D2 receptor gene; 5'-TCTGTGCCATCAGCATAGACAGGT-3' (sense) and 5'-TAAAGCCAAACAGAAGAGGGCAGG-3' (antisense) for the dopamine D3 receptor gene; 5'-TCTTCGTCTACTCCGAGGTCCA-3' (sense) and 5'-TGATGGCGCACAGGTTGAAGAT-3' (antisense) for the dopamine D4 receptor gene; 5'-GCCAAGGTCATCCATGACAACTTTGG-3' (sense) and 5'-GCCTGCTTCACCACCTTCTTGATGTC-3' (antisense) for *GAPDH*. The PCR amplification products were separated by electrophoresis in an agarose gel and stained using ethidium bromide.

Quantification of reactive oxygen species (ROS)

The generation of intracellular ROS was detected using CellROX, a fluorescence probe. After exposure to pimozide at different concentrations for 24 h, the cells were incubated with the CellROX Green reagent (Thermo Fisher Scientific, Waltham, MA, USA) for 60 min in the dark and washed with phosphate-buffered saline. The changes in CellROX Green-induced fluorescence were analyzed using an SH800 Flow Cytometer (Sony Biotechnology Inc., Tokyo, Japan).

Western blot analysis

The cultured cells were lysed using a lysis buffer containing 62.5 mM Tris-HCl (pH 6.8) (Nacalai Tesque, Inc.), 2% sodium dodecyl sulfate (SDS; Nacalai Tesque, Inc.), 10% glycerol (Nacalai Tesque, Inc.), 6% 2-mercaptoethanol (Nacalai Tesque, Inc.) and 0.01% bromophenol blue (Wako Pure Chemical Industries). After protein quantitation using the DC Protein Assay kit (Bio-Rad Laboratories, Inc., Hercules, CA, USA), the cell lysates (20 mg) from each sample were resolved using SDS-polyacrylamide gel electrophoresis prior to their transfer to polyvinylidene difluoride membranes (Merck KGaA, Darmstadt, Germany) and probing with primary antibodies (1:1,000). The blots were then incubated with horseradish peroxidase-conjugated secondary anti-mouse (1:1,000; Cell Signaling Technology, Inc., Beverly, MA, USA) or anti-rabbit (1:1,000; Cell Signaling Technology, Inc.) IgGs. Immunoreactivity was quantified using an enhanced chemiluminescence reagent (Amersham Biosciences Corp., Piscataway, NJ, USA). The antibodies against Bcl-2, Bcl-xL, Bax, cellular inhibitor of apoptosis (c-IAP) 1, survivin, histone H2AX, phospho-H2AX (Ser139), activating transcription factor (ATF) 4, STAT3, phospho-STAT3 (Tyr705), STAT5, phospho-STAT5 (Tyr694), phospho-IkBa (Ser32/36), IκB kinase (IKK) a, IKKb, phospho-IKKa/b (Ser176/180 and Ser177/181), Akt, phospho-Akt (Thr308), phospho-Akt (Ser473), cleaved poly(ADP-ribose) polymerase (PARP), ae well as cleaved caspase-8, caspase-9 and caspase-3 were obtained from Cell Signaling Technology, Inc. Antibodies against cyclin E, cyclin-dependent kinase (CDK) 2, CDK4, CDK6, p21, p53 and actin were obtained from Neomarkers, Inc. (Fremont, CA, USA). Antibodies against the X-linked inhibitor of apoptosis protein (XIAP) and phospho-retinoblastoma protein (pRb) (Ser780) were obtained from Medical & Biological Laboratories, Co. Antibodies against cyclin D2, p27, myeloid cell leukemia-1 (Mcl-1), c-IAP2, GADD45a, IkBa, JunB and JunD were purchased from Santa Cruz Biotechnology, Inc. (Dallas, TX, USA). An antibody specific for c-Myc was obtained from Wako Pure Chemical Industries.

Xenograft tumor model

HUT-102 cell suspensions (1×10^7/0.2 ml of RPMI-1640 medium) were injected subcutaneously into 5-week-old female C.B-17/Icr-severe combined immunodeficient (SCID) mice (Japan SLC, Inc., Hamamatsu, Japan) on day 0. The mice were randomly divided into control and treatment groups (n = 9, each). Either pimozide (25 mg/kg) or a solvent (0.5% methylcellulose, Wako Pure Chemical Industries) was administered via oral gavage five times per week between days 1 and 28. The tumor size was measured weekly using shifting calipers to calculate the tumor volume using the following formula: $p/6 \times h \times l \times w$ [8]. The body weight of each mice was also measured weekly. At the time of sacrifice on day 28, the xenograft tumors and blood samples were collected rapidly. The weight of each tumor was measured, and the sera were stored at −80 °C until they were assayed for human soluble interleukin-2 receptor a (sIL-2Ra). The studies were approved by the Animal Care and Use Committee at the University of the Ryukyus (A2019149).

Measurement of serum sIL-2Ra levels

The serum sIL-2Ra levels were measured in mice treated or untreated with pimozide using enzyme-linked immunosorbent assay (ELISA) for human sIL-2Ra (Diaclone SAS, Besançon, France) in accordance with the manufacturer's instructions.

Statistical analysis

Data are presented as the mean ± standard deviation (SD). Statistical analysis was performed using a Student's *t*-test or ANOVA along with the Tukey-Kramer test. Differences were considered significant at $P < 0.05$.

Results

HTLV-1-infected T cells were sensitive to pimozide

The treatment of HTLV-1-infected T cells with pimozide at various concentrations for up to 72 h inhibited cell proliferation and survival in a dose- and time-dependent manner, as indicated by the reduction in WST-8 activity (Fig. 1a). As a negative control for ATL, uninfected T cells were also treated with pimozide. There were limited effects exerted on the proliferation and survival of uninfected T cells (Fig. 1b). Since pimozide is an antagonist of the dopamine D2 receptor subfamily (D2, D3 and D4) [6], we analyzed the expression of dopamine receptors on T cells. RT-PCR analysis revealed that the D2, D3 or D4 receptors were not expressed in uninfected T cells, whereas they were expressed in all HTLV-1-infected T cells (Fig. 1c). There findings indicated that pimozide, which is a potent dopamine D2 receptor subfamily antagonist, inhibits the proliferation and survival of HTLV-1 infected T cells, and the expression of the dopamine D2 receptor subfamily could be associated with the inhibitory effect to an extent.

Effects of pimozide on the cell cycle in HTLV-1-infected T cells

To determine whether pimozide inhibits cell cycle progression to suppress cell proliferation, the effect of pimozide on cell cycle distribution was analyzed using PI staining. After MT-2 and HUT-102 cells were treated with pimozide at the indicated concentrations for 24 h, the number of cells in the G1 phase increased, whereas the number of cells in the S phase decreased compared to the number of untreated cells (Fig. 2a). The western blotting results showed the reduced expression of the cell cycle markers cyclin D2, cyclin E, CDK2, CDK4 and CDK6, along with increased expression of p21, p27 and p53 (Fig. 2b), which is consistent with the G1 arrest observed in the flow cytometric analysis. Pimozide also downregulated c-Myc expression and induced pRb dephosphorylation (Fig. 2b). These results indicated that pimozide hindered cell proliferation in association with the inhibition of G_1–S progression.

Induction of apoptosis and necroptosis in HTLV-1-infected T cells treated with pimozide

Next, we investigated whether pimozide treatment induced apoptosis in HTLV-1-infected T cells. The microscopic examination of pimozide-treated MT-2 and HUT-102 cell nuclei after Hoechst 33342 staining revealed striking morphological changes, with the cells exhibiting apoptotic characteristics, along with nuclear fragmentation and chromatin condensation (Fig. 3a). The apoptotic effects induced by pimozide on HTLV-1-infected T cells were also analyzed by APO2.7 staining using flow cytometry [7]. Pimozide was observed to induce apoptosis in MT-2, HUT-102 and MT-4 cells (Fig. 3b). Pimozide induced the cleavage of a known caspase-3 substrate, PARP, as well as of caspase-3, caspase-8 and caspase-9 in a dose-

dependent manner (Fig. 3c), thus unveiling the role of caspase in pimozide-induced apoptosis. Furthermore, caspase-3, -8 and -9 activity levels were measured in cells treated with pimozide (Fig. 3d). This experiment also demonstrated the activation of the three caspases (Fig. 3d). To evaluate the role of caspase-dependent cell death, the broad-range caspase inhibitor z-VAD-FMK was used to selectively inhibit the apoptotic pathway. As shown in Fig 4a, HUT-102 and MT-4 cells were pretreated with z-VAD-FMK for 2 h, followed by incubation with pimozide for 24 h. z-VAD-FMK reduced the pimozide-induced inhibition of cell viability in the WST-8 assay partially but significantly. These results demonstrated the prevalence of apoptosis while also indicating the involvement of caspase-independent cell death.

Besides apoptosis, another mode of programmed cell death, necroptosis, has also been identified [9]. We further evaluated whether necroptosis is required for the induction of cell death by pimozide. Pimozide-induced cell death was reduced in the presence of the necroptosis inhibitor necrostatin-1 (Fig. 4b). These results indicated that apoptosis and necroptosis are involved in pimozide-triggered cell death.

Pimozide induced ROS accumulation

ROS accumulation could partially contribute to cell apoptosis and necroptosis [10, 11]. We evaluated the effect of pimozide on the ROS levels in MT-2 and HUT-102 cells. Flow cytometry experiments revealed the elevation in ROS production in cells after pimozide treatment (Fig. 5a). To determine whether the generation of ROS induced by pimozide was related to its ability to induce the apoptosis of HTLV-1-infected T cells, we analyzed the apoptotic effects induced by pimozide in the presence of the ROS scavenger NAC. As shown in Fig. 5b, NAC impeded the pimozide-mediated induction of apoptosis.

Modulation of apoptotic regulatory protein expression in pimozide-induced apoptosis

The balance between pro-apoptotic and anti-apoptotic proteins eventually determines whether cells will undergo apoptosis or survive. We evaluated whether pimozide induces cell death by modulating the expression of Bcl-2 and IAP family members, which eventually determine the cell response to apoptotic stimuli. As shown in Fig. 5c, pimozide treatment caused the downregulation of Bcl-xL, Mcl-1, c-IAP2, XIAP and survivin; conversely, it induced the expression of the pro-apoptotic protein Bax. These results indicated that Bcl-2 and IAP family proteins may be involved in pimozide-induced apoptosis.

When produced in excess, ROS can induce extensive damage in DNA, proteins and lipids [10]. To evaluate whether the cytotoxic response induced by pimozide is mediated via DNA damage and/or whether the increased ROS levels caused oxidative damage to DNA, the levels of phosphorylated H2AX, which is a DNA damage marker, and the expression of the DNA damage-inducible protein GADD45a were assessed. As postulated, the expression of phosphorylated H2AX and GADD45a was upregulated in cells treated with pimozide (Fig. 5c).

The proper functioning of the endoplasmic reticulum (ER) is essential for most cellular activities as well as for survival. ER stress leads to mitochondrial dysfunction and apoptosis [12]. ROS is known to

induce ER stress-dependent apoptosis [10]. The involvement of ER stress in pimozide-induced cell apoptosis was investigated. The levels of ATF4, an ER stress marker, increased in response to pimozide treatment (Fig. 5c). The results indicated that ER stress signaling is one of the potential pathways involved in the induction of apoptosis.

Pimozide suppresses the activities of STAT3/5, NF-κB, Akt and AP-1

STAT3/5 act as signaling mediators involved in cell growth and survival. Both are constitutively activated in ATL, and STAT activation is associated with cell cycle progression [13]. Çyclin D2, c-Myc, Bcl-xL and Mcl-1 are regulated by STAT3/5 [14]. Therefore, agents that target STAT3/5 could be useful for the treatment of ATL. Since pimozide has been reported to inhibit STAT3/5 activation [15, 16], we assessed the effect exerted by pimozide on STAT3/5 activity in HTLV-1 infected T cells, in which both proteins are activated. Pimozide was observed to inhibit STAT3/5 phosphorylation (Fig. 6a). The NF-κB, Akt and AP-1 pathways, which are common cell survival pathways, are also constitutively activated in HTLV-1-infected T cells [17,18]. As shown in Fig. 6a, pimozide suppressed the phosphorylation of IkBa and its upstream kinases IKKa/b, whereas it enhanced the expression of IkBa. In addition, pimozide treatment decreased the levels of Akt phosphorylation (Fig. 6a). AP-1 is a dimeric transcription factor composed of proteins belonging to the Jun, Fos and ATF protein families [18]. JunB and JunD were expressed at high levels and mediated AP-1 DNA-binding activity in HTLV-1-infected T cells [18–20]. JunB and JunD expression was also reduced upon treatment with pimozide (Fig. 6a). Therefore, in addition to STAT3/5, the NF-κB, Akt and AP-1 pathways were suppressed via the dephosphorylation of IKKα/β, IκBα and Akt as well as via the inhibition of JunB and JunD expression, in response to pimozide treatment in HTLV-1-infected T cells.

Pimozide inhibited the growth of ATL xenografts in SCID mice

Lastly, we evaluated the antitumor effects of pimozide on the growth of HTLV-1-infected T cell HUT-102 xenografted tumors in vivo. The tumor volumes in mice from the untreated control group increased, whereas the tumor volumes reduced by 32%, a significant reduction ($P < 0.05$), in mice from the treated group (Fig. 6b). The tumor weight decreased in mice treated with pimozide (Fig. 6d). Notably, pimozide treatment was well-tolerated, and no significant effects were exerted on body weight (Fig. 6c). Furthermore, the serum biomarker levels were assessed using ELISA. Pimozide treatment reduced the levels of sIL-2Ra; however, the differences were not statistically significant (Fig. 6e). These results implied that pimozide exhibits anti-ATL activities in vivo without generating significant side effects.

Discussion

Several epidemiological studies and clinical data have shown a lower rate of cancer incidence among patients with schizophrenia, and medication used to treat schizophrenia may be the possible mediators of this effect [4]. While pimozide is a neuroleptic drug with manageable side effects in clinical use, it exhibits therapeutic effects in certain types of cancer [6]. Pimozide has also shown efficacy in the treatment of metastatic melanoma and has been shown to be well-tolerated in clinical trials [21, 22]. In addition, no hematological toxicity ascribable to pimozide has been reported [16]. In this study, we

investigated the cytotoxic effects of pimozide and showed that pimozide could be used as a novel anti-ATL drug, based on its ability to suppress cell proliferation and increase cell death in selectively HTLV-1-infected T cells in vitro and to inhibit tumor growth in xenografts in vivo.

Pimozide inhibited cell proliferation of HTLV-1-infected T cells as a result of G1 cell cycle arrest and downregulated expression of cyclin D2, cyclin E, CDK2, CDK4, CDK6 and c-Myc along with increased expression of p21, p27 and p53. Cyclin D2-CDK4/6 and cyclin E-CDK2 induce pRb phosphorylation, which initiates DNA synthesis. p21 and p27 inhibit cyclin-CDK complexes. c-Myc induces the expression of cyclin D2, cyclin E, CDK2, CDK4 and CDK6. Moreover, c-Myc represses p21 and p27 expression [23]. The pimozide-induced reduction in cyclin and CDK levels and increase in p21 and p27 levels may be partially attributed to the downregulation of c-Myc, which results in pRb dephosphorylation.

Pimozide promoted the apoptosis of HTLV-1-infected T cells and increased ROS generation. In several studies, ROS generation has been associated with apoptosis and necroptosis induction [10, 11]. NAC, a ROS scavenger, suppressed pimozide-induced apoptosis, indicating that the anti-ATL effect of pimozide was linked to ROS generation. Moreover, pimozide cytotoxicity was impacted by pan-caspase or necroptosis inhibition. These results indicated that apoptosis and necroptosis are involved in the pimozide-induced elimination of HTLV-1-infected T cells.

At elevated levels, ROS can cause extensive DNA damage [10]. Pimozide also exerts genotoxic effects on DNA by promoting DNA double-strand breaks, which corresponds to an increase in the phosphorylation of histone H2AX [24]. ROS also activate p53, which regulates multiple signaling pathways triggered by cellular stress, inducing either cell cycle arrest or apoptosis [10, 25, 26]. Pimozide was shown to induce p53 expression. Upon induction, p53 influences downstream genes, including *p21* and *GADD45α*, to promote cell cycle arrest and DNA damage. p53 also regulates apoptosis by downregulating pro-survival proteins, such as members of the Bcl-2 family and the IAP family, and by upregulating pro-apoptotic proteins [25, 26]. Previous studies have shown that ROS plays an essential role in ER stress induced by various antitumor agents [27]. In addition, p53 also triggers ER stress [28]. Pimozide treatment induced the expression of the ER stress marker ATF4. These results implied that pro-apoptotic ER stress also contributes to cell death induced by pimozide. Pimozide induces cell cycle arrest and cell death via a ROS-mediated p53-regulated stress pathway.

Multiple signaling pathways, including STATs, NF-κB, Akt and AP-1 signaling, are essential for the pathogenesis of ATL, as these pathways directly or indirectly regulate the expression of genes that induce or maintain the proliferation and survival of ATL cells [13, 17, 18]. Therefore, these signaling pathways are attractive targets for ATL therapy. Previous studies have shown that pimozide exerts anti-neoplastic effects by suppressing STAT3/5 activity [15, 16]. We confirmed that the anti-ATL effects of pimozide were related to STAT3/5 suppression, as reported previously [15, 16]. Pimozide was also shown to act as a potent anti-ATL agent by inhibiting the NF-κB, Akt and AP-1 signaling pathways. Pimozide impacted the NF-κB and Akt signaling pathways by inhibiting IκBα, IKKα/β and Akt phosphorylation. Furthermore, pimozide suppressed AP-1 signaling by inhibiting JunB and JunD expression. We also observed the

effects exerted by pimozide on NF-κB, AP-1, Akt and STAT3/5 signaling by measuring protein expression from the target genes. Pimozide treatment of HTLV-1-infected T cells downregulated the expression of their target proteins, including cyclin D2/E, CDK2/4/6, c-Myc, Bcl-xL, Mcl-1, c-IAP2, XIAP and survivin, which indicates the inactivation of these pathways [14, 29 – 36]. Therefore, we propose that pimozide suppresses the proliferation of HTLV-1-infected T cells by inhibiting the NF-κB, AP-1, Akt and STAT3/5 pathways. The results of the present study indicated that the concurrent blockade of these pathways may be effective in suppressing cell proliferation.

Notably, the cytotoxic effects of pimozide appeared to be specific to HTLV-1-infected T cells, as the proliferation and survival of uninfected T cells remained unaffected by pimozide administration at concentrations below 5 μM. Since pimozide is an antagonist of the dopamine D2 receptor subfamily, we evaluated the expression of these receptors in HTLV-1-infected T cells and found that the levels of the dopamine D2 receptor subfamily mRNA were elevated compared to the corresponding levels in uninfected T cells. In future, further studies should be conducted to evaluate the association between the expression of these receptors and the anti-ATL effects exerted by pimozide. Although studies using fresh leukemic cells obtained from ATL patients are required to evaluate pimozide as an anti-ATL agent, pimozide treatment was found to be well-tolerated in a murine ATL model, with no significant effects exerted on body weight. In conclusion, the present study provides compelling evidence that pimozide demonstrates anti-ATL activity via multiple molecular mechanisms, and could therefore be considered a novel candidate for ATL treatment.

Declarations

Consent for publication

All authors consent to the publication pf this study.

Availability of data and materials

The data and materials used in this study are available from the corresponding author on reasonable request.

Competing interests

No potential competing interest is reported by the authors.

Funding

The present study was supported in part by JSPS KAKENHI (17K07175).

Authors' contributions

Conceptualization: Naoki Mori; Methodology: Chie Ishikawa and Naoki Mori; Formal analysis and investigation: Chie Ishikawa and Naoki Mori; Writing: Naoki Mori; Funding acquisition: Chie Ishikawa;

Resources: Naoki Mori; Supervision: Naoki Mori.

Acknowledgments

The authors express their gratitude to the Fujisaki Cell Center, Hayashibara Biochemical Laboratories, Inc. for providing HUT-102, MT-1 and Jurkat cells, to Dr. Naoki Yamamoto (Tokyo Medical and Dental University) for providing MT-2, MT-4 and MOLT-4 cells, to Dr. Masahiro Fujii (Niigata University) for providing TL-Oml and CCRF-CEM cells, and to Dr. Diane Prager (UCLA School of Medicine) for providing SLB-1 cells. Protein concentration measurement and flow cytometry analyses were performed at the University of the Ryukyus Center for Research Advancement and Collaboration. We would like to thank Editage (www.editage.com) for their assistance with English language editing.

Compliance with ethical standards

Conflict of interest

No potential conflict of interest is reported by the authors.

Research involving animals

All animal experiments were approved by the Animal Care and Use Committee at the University of the Ryukyus (A2019149).

Informed consent

Not applicable.

References

1. Iwanaga M, Watanabe T, Yamaguchi K (2012) Adult T-cell leukemia: a review of epidemiological evidence. Front Microbiol 3:322
2. Nasr R, Marçais A, Hermine O, Bazarbachi A (2017) Overview of targeted therapies for adult T-cell leukemia/lymphoma. Methods Mol Biol 1582:197–216
3. Ishitsuka K, Tamura K (2014) Human T-cell leukaemia virus type I and adult T-cell leukaemia-lymphoma. Lancet Oncol 15:e517–e526
4. Mortensen PB (1989) The incidence of cancer in schizophrenic patients. J Epidemiol Community Health 43:43–47
5. Wiklund ED, Catts VS, Catts SV, Ng TF, Whitaker NJ, Brown AJ, Lutze-Mann LH (2010) Cytotoxic effects of antipsychotic drugs implicate cholesterol homeostasis as a novel chemotherapeutic target. Int J Cancer 126:28–40
6. Elmaci I, Altinoz MA (2018) Targeting the cellular schizophrenia. Likely employment of the antipsychotic agent pimozide in treatment of refractory cancers and glioblastoma. Crit Rev Oncol

Hematol 128:96–109

7. Zhang C, Ao Z, Seth A, Schlossman SF (1996) A mitochondrial membrane protein defined by a novel monoclonal antibody is preferentially detected in apoptotic cells. J Immunol 157:3980–3987
8. Tomayko MM, Reynolds CP (1989) Determination of subcutaneous tumor size in athymic (nude) mice. Cancer Chemother Pharmacol 24:148–154
9. Grootjans S, Vanden Berghe T, Vandenabeele P (2017) Initiation and execution mechanisms of necroptosis: an overview. Cell Death Differ 24:1184–1195
10. Redza-Dutordoir M, Averill-Bates DA (2016) Activation of apoptosis signalling pathways by reactive oxygen species. Biochim Biophys Acta 1863:2977–2992
11. Hsu S-K, Chang W-T, Lin I-L, Chen Y-F, Padalwar NB, Cheng K-C, Teng Y-N, Wang C-H, Chiu C-C (2020) The role of necroptosis in ROS-mediated cancer therapies and its promising applications. Cancers (Basel) 12:2185
12. Tabas I, Ron D (2011) Integrating the mechanisms of apoptosis induced by endoplasmic reticulum stress. Nat Cell Biol 13:184–190
13. Takemoto S, Mulloy JC, Cereseto A, Migone TS, Patel BK, Matsuoka M, Yamaguchi K, Takatsuki K, Kamihira S, White JD, Leonard WJ, Waldmann T, Franchini G (1997) Proliferation of adult T cell leukemia/lymphoma cells is associated with the constitutive activation of JAK/STAT proteins. Proc Natl Acad Sci USA 94:13897–13902
14. Verhoeven Y, Tilborghs S, Jacobs J, De Waele J, Quatannens D, Deben C, Prenen H, Pauwels P, Trinh XB, Wouters A, Smits ELJ, Lardon F, van Dam PA (2020) The potential and controversy of targeting STAT family members in cancer. Semin Cancer Biol 60:41–56
15. Gonçalves JM, Silva CAB, Rivero ERC, Cordeiro MMR (2019) Inhibition of cancer stem cells promoted by Pimozide. Clin Exp Pharmacol Physiol 46:116–125
16. Nelson EA, Walker SR, Weisberg E, Bar-Natan M, Barrett R, Gashin LB, Terrell S, Klitgaard JL, Santo L, Addorio MR, Ebert BL, Griffin JD, Frank DA (2011) The STAT5 inhibitor pimozide decreases survival of chronic myelogenous leukemia cells resistant to kinase inhibitors. Blood 117:3421–3429
17. Mori N (2009) Cell signaling modifiers for molecular targeted therapy in ATLL. Front Biosci 14:1479–1489
18. Gazon H, Barbeau B, Mesnard J-M, Peloponese J-M Jr (2018) Hijacking of the AP-1 signaling pathway during development of ATL. Front Microbiol 8:2686
19. Nakayama T, Hieshima K, Arao T, Jin Z, Nagakubo D, Shirakawa AK, Yamada Y, Fujii M, Oiso N, Kawada A, Nishio K, Yoshie O (2008) Aberrant expression of Fra-2 promotes CCR4 expression and cell proliferation in adult T-cell leukemia. Oncogene 27:3221–3232
20. Ishikawa C, Senba M, Mori N (2020) Evaluation of artesunate for the treatment of adult T-cell leukemia/lymphoma. Eur J Pharmacol 872:172953
21. Taub RN, Baker MA (1979) Treatment of metastatic malignant melanoma with pimozide. Lancet 1:605

22. Neifeld JP, Tormey DC, Baker MA, Meyskens FL Jr, Taub RN (1983) Phase II trial of the dopaminergic inhibitor pimozide in previously treated melanoma patients. Cancer Treat Rep 67:155–157
23. Bretones G, Delgado MD, León J (2015) Myc and cell cycle control. Biochim Biophys Acta 1849:506–516
24. Celeste A, Petersen S, Romanienko PJ, Fernandez-Capetillo O, Chen HT, Sedelnikova OA, Reina-San-Martin B, Coppola V, Meffre E, Difilippantonio MJ, Redon C, Pilch DR, Olaru A, Eckhaus M, Camerini-Otero RD, Tessarollo L, Livak F, Manova K, Bonner WM, Nussenzweig MC, Nussenzweig A (2002) Genomic instability in mice lacking histone H2AX. Science 296:922–927
25. Aubrey BJ, Kelly GL, Janic A, Herold MJ, Strasser A (2018) How does p53 induce apoptosis and how does this relate to p53-mediated tumour suppression? Cell Death Differ 25:104–113
26. Goldar S, Khaniani MS, Derakhshan SM, Baradaran B (2015) Molecular mechanisms of apoptosis and roles in cancer development and treatment. Asian Pac J Cancer Prev 16:2129–2144
27. Verfaillie T, Garg AD, Agostinis P (2013) Targeting ER stress induced apoptosis and inflammation in cancer. Cancer Lett 332:249–264
28. Gong C, Yang Z, Zhang L, Wang Y, Gong W, Liu Y (2017) Quercetin suppresses DNA double-strand break repair and enhances the radiosensitivity of human ovarian cancer cells via p53-dependent endoplasmic reticulum stress pathway. Onco Targets Ther 11:17–27
29. Pahl HL (1999) Activators and target genes of Rel/NF-κB transcription factors. Oncogene 18:6853–6866
30. Wang C-Y, Mayo MW, Korneluk RG, Goeddel DV, Baldwin AS Jr (1998) NF-κB antiapoptosis: induction of TRAF1 and TRAF2 and c-IAP1 and c-IAP2 to suppress caspase-8 activation. Science 281:1680–1683
31. Iwanaga R, Ohtani K, Hayashi T, Nakamura M (2001) Molecular mechanism of cell cycle progression induced by the oncogene product Tax of human T-cell leukemia virus type I. Oncogene 20:2055–2067
32. Iwanaga R, Ozono E, Fujisawa J, Ikeda MA, Okamura N, Huang Y, Ohtani K (2008) Activation of the *cyclin D2* and *cdk6* genes through NF-κB is critical for cell-cycle progression induced by HTLV-I Tax. Oncogene 27:5635–5642
33. Kawakami H, Tomita M, Matsuda T, Ohta T, Tanaka Y, Fujii M, Hatano M, Tokuhisa T, Mori N (2005) Transcriptional activation of survivin through the NF-κB pathway by human T-cell leukemia virus type I tax. Int J Cancer 115:967–974
34. Hess J, Angel P, Schorpp-Kistner M (2004) AP-1 subunits: quarrel and harmony among siblings. J Cell Sci 117:5965–5973
35. Reuter S, Prasad S, Phromnoi K, Ravindran J, Sung B, Yadav VR, Kannappan R, Chaturvedi MM, Aggarwal BB (2010) Thiocolchicoside exhibits anticancer effects through downregulation of NF-κB pathway and its regulated gene products linked to inflammation and cancer. Cancer Prev Res 2010 3:1462–1472

36. Zheng H-C (2017) The molecular mechanisms of chemoresistance in cancers. Oncotarget 8:59950–59964

Figures

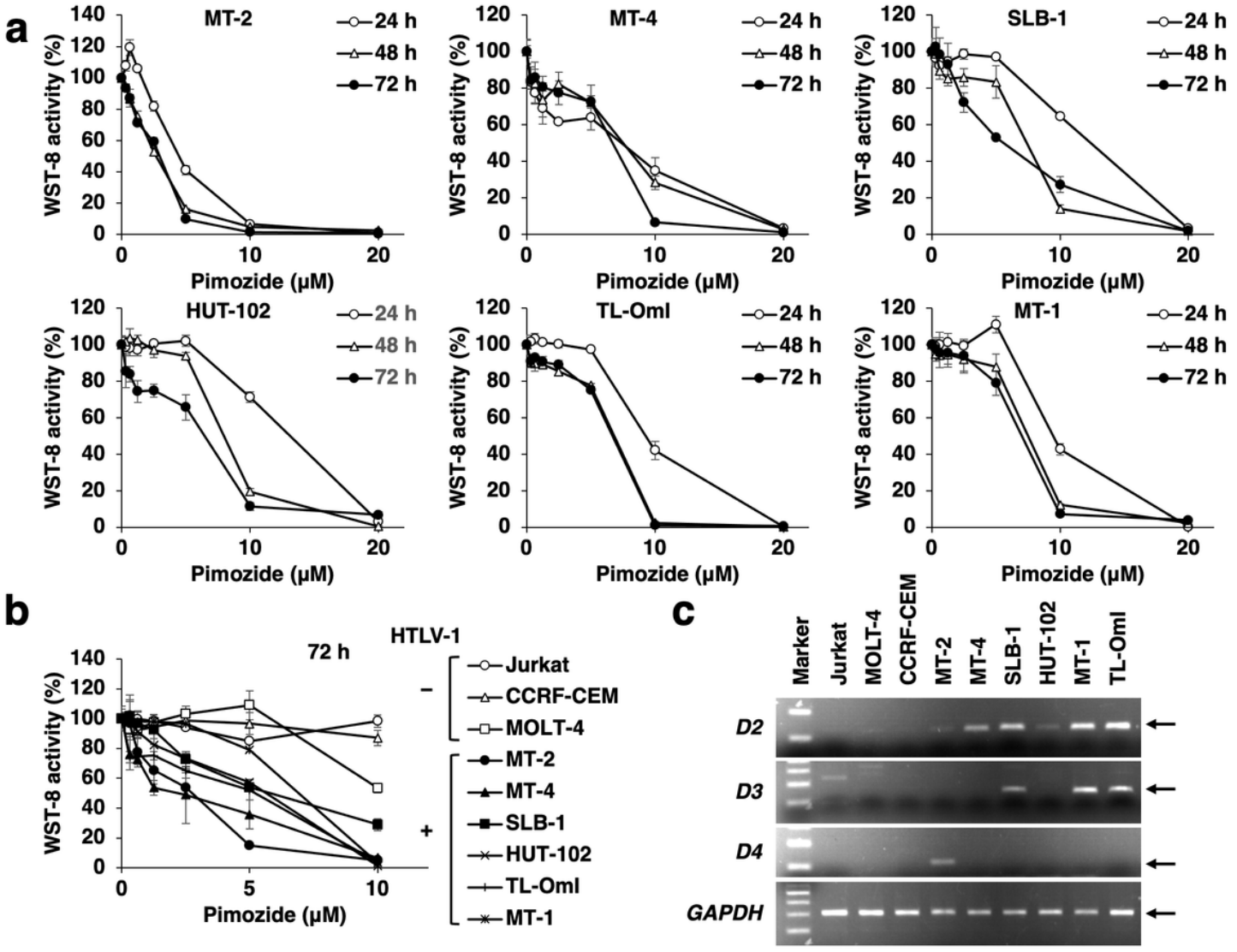

Figure 1

Inhibition of cell growth and viability by pimozide, and mRNA expression of the dopamine D2 receptor subfamily in T cells. a. Pimozide inhibits cell growth and viability in a dose- and time-dependent manner. HTLV-1-infected T cells were treated with pimozide at different concentrations for 24–72 h, and were then subjected to a WST-8 colorimetric assay to assess their growth and viability. b. Sensitivity of HTLV-1-infected and -uninfected T cells to pimozide. WST-8 activity of multiple T cell lines after treatment with pimozide at different doses for 72 h. Data are presented as the mean ± SD from triplicate cultures. c. Expression of dopamine D2 receptor subfamily mRNA in T cells was measured using RT-PCR. GAPDH was used as an internal control.

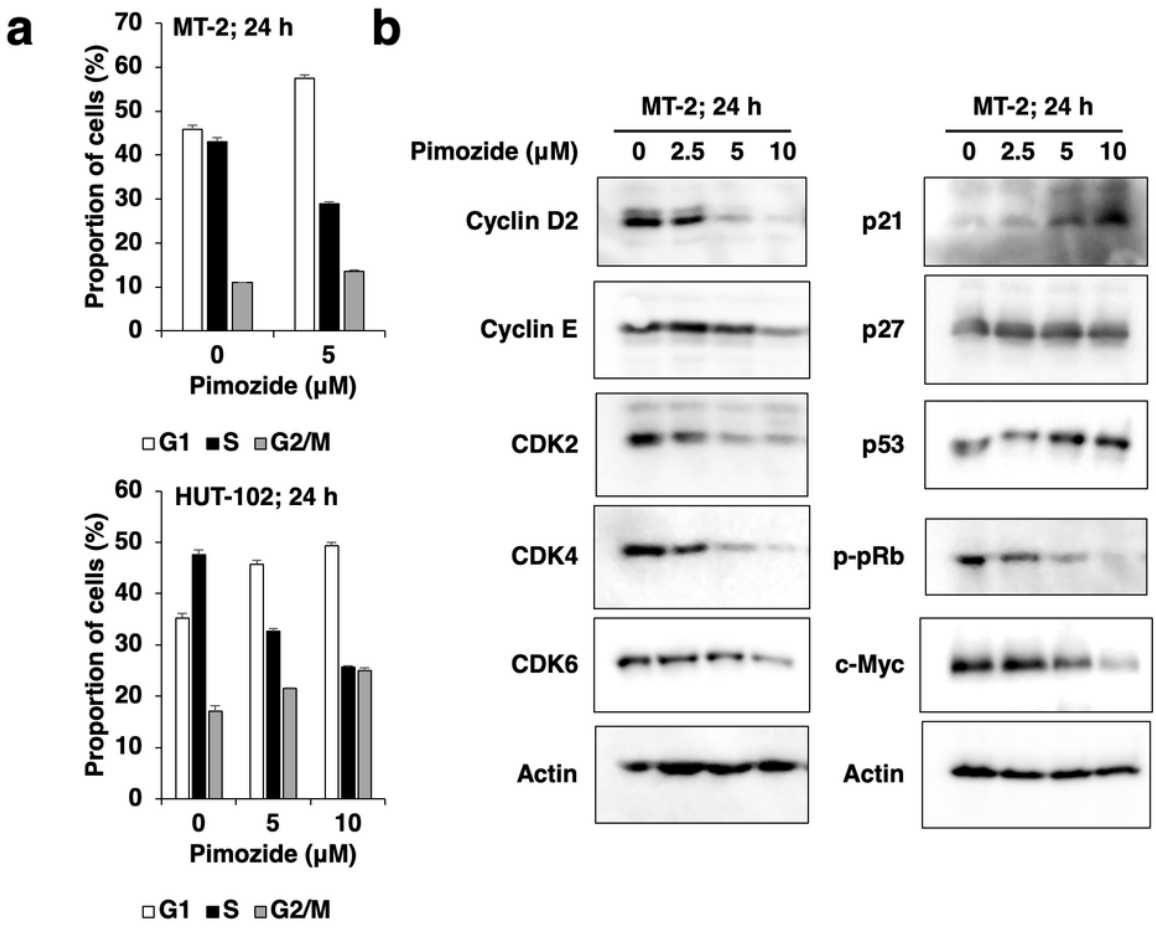

Figure 2

Cell cycle arrest of HTLV-1-infected T cells induced by pimozide. a. Pimozide interrupts cell cycle progression at the G1 phase. MT-2 and HUT-102 cells were cultured in the absence or presence of pimozide at the indicated concentrations for 24 h and subjected to PI staining and flow cytometry to determine the percentage of cells in each cell cycle phase. Data are presented as the mean ± SD from triplicate cultures. b. Pimozide treatment affected the expression of cell cycle regulatory proteins. MT-2 cells were treated with pimozide at the indicated concentrations for 24 h and harvested. The protein samples were subjected to immunoblotting analysis for the expression of cell cycle regulatory proteins. Actin was used as the loading control.

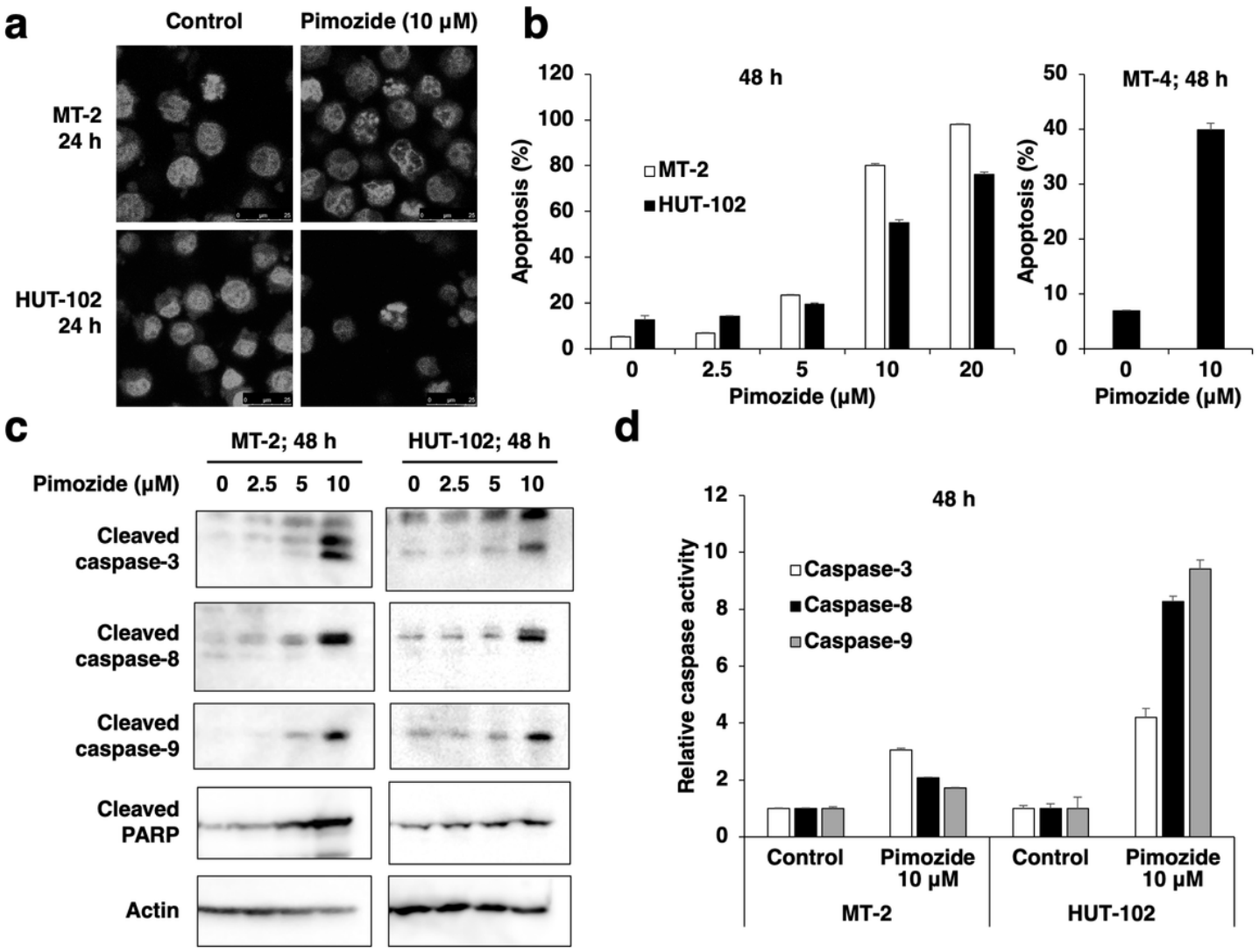

Figure 3

Pimozide-induced apoptosis in HTLV-1-infected T cells. a. MT-2 and HUT-102 cells were treated with 10 μM pimozide for 24 h. Cell nuclei were stained with Hoechst 33342 and observed under a DMI6000 microscope. b. Flow cytometric observation of apoptosis in HTLV-1-infected T cells treated with pimozide at the indicated concentrations for 48 h. The percentage of apoptosis in HTLV-1-infected T cells was determined using APO.2.7 staining and flow cytometry analysis. Data are presented as the mean ± SD from triplicate cultures. c. Western blot analysis of the levels of cleaved caspases and PARP. MT-2 and HUT-102 cells were treated with pimozide at the indicated concentrations for 48 h. The cell lysates were subjected to western blot analysis. Actin was used as a loading control. d. Activated caspases in pimozide-treated cells. MT-2 and HUT-102 cells were cultured with 10 μM pimozide for 48 h. Cell lysates were subjected to a colorimetric caspase assay for quantification of caspase activity. Data are presented as the mean ± SD from triplicate cultures.

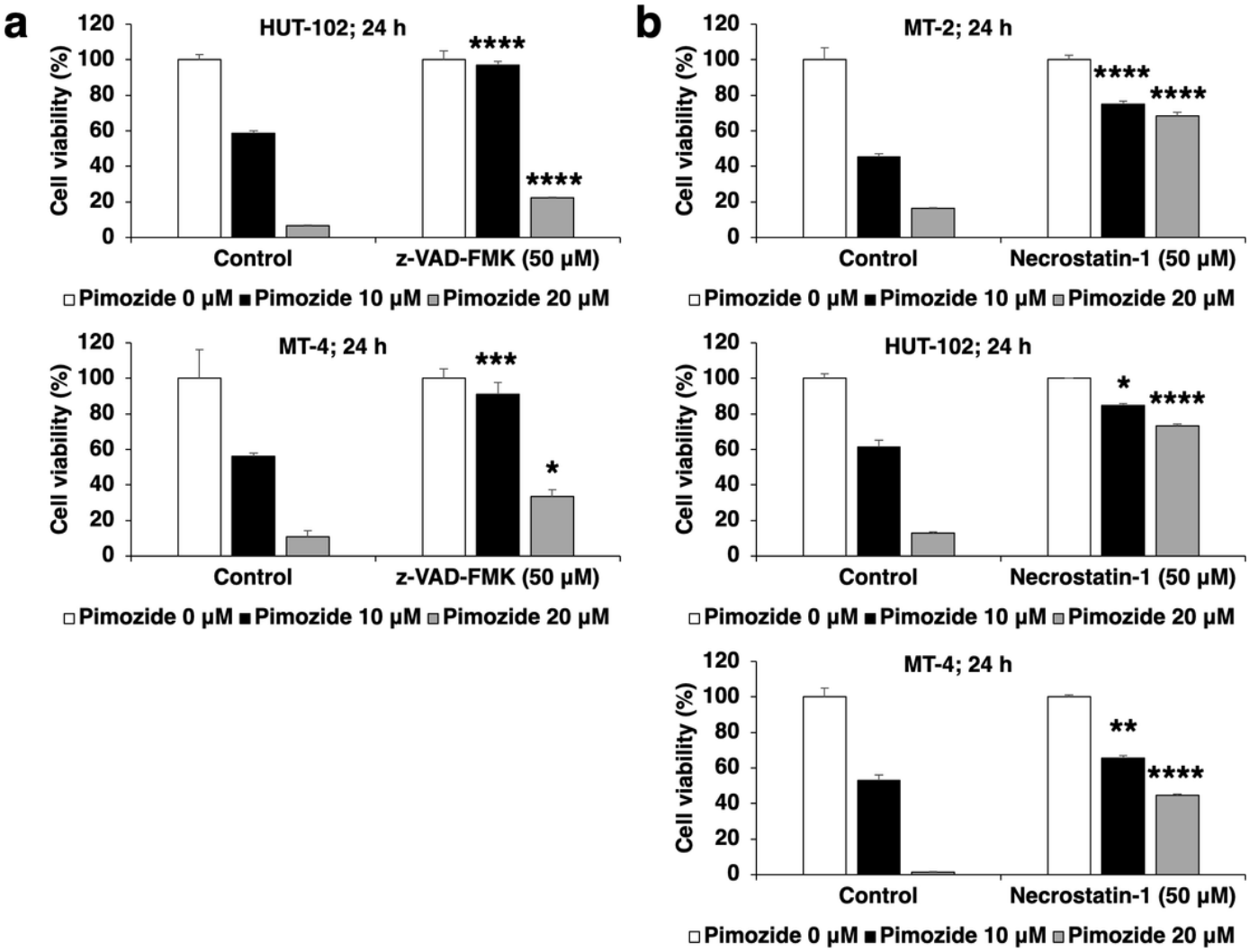

Figure 4

Pimozide-induced cell death. Cells were pretreated with 50 μM z-VAD-FMK (a) or necrostatin-1 (b) for 2 h. After pretreatment, pimozide was administered at the indicated concentrations, followed by treatment for 24 h. Thereafter, cytotoxicity was assessed using the WST-8 assays. Data are presented as the mean ± SD from triplicate cultures. *P < 0.001, **P < 0.005, ***P < 0.0005 and ****P < 0.0001 compared to controls (pimozide alone).

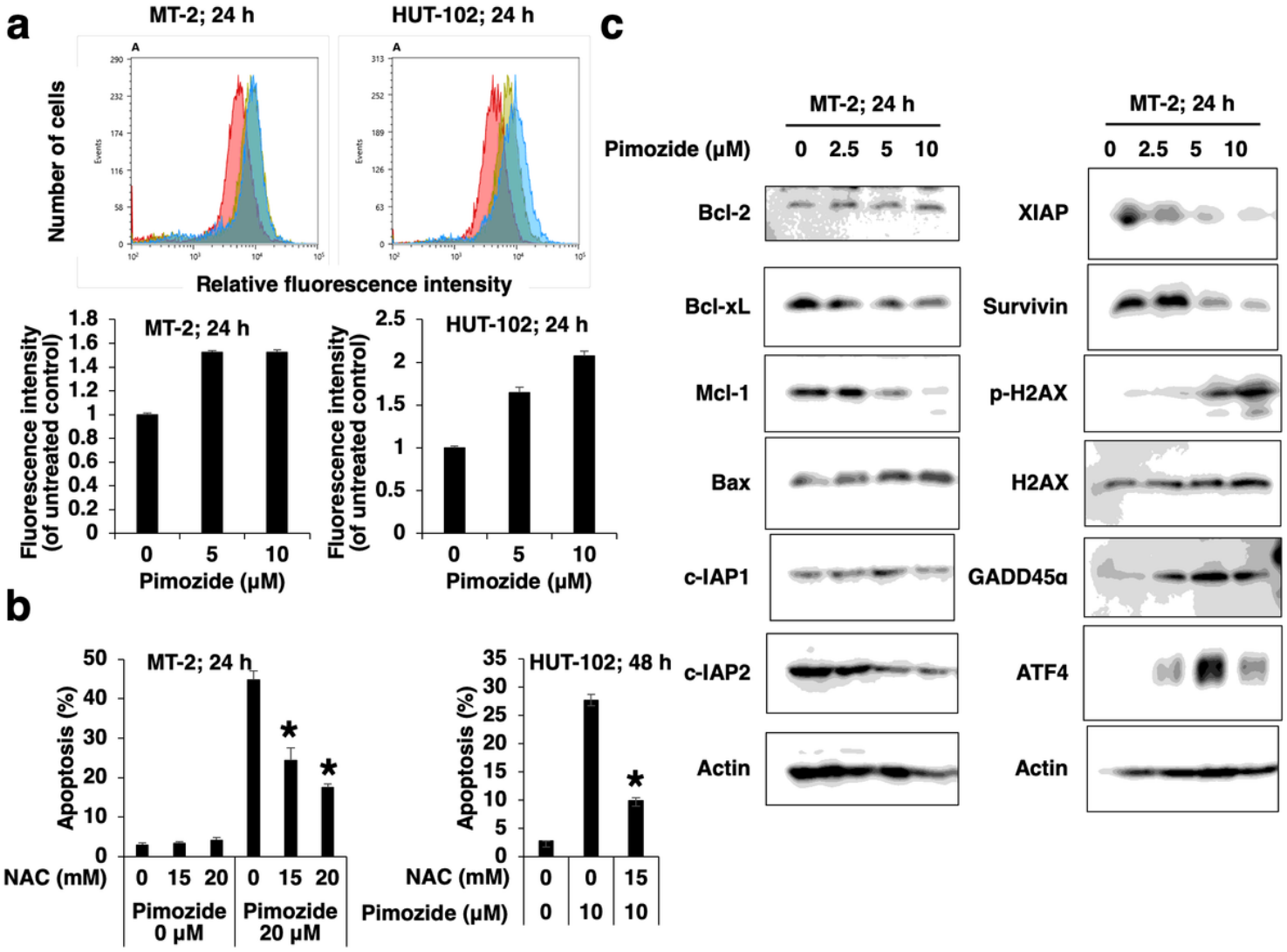

Figure 5

ROS triggers apoptosis by altering the expression of apoptosis-related proteins in pimozide-treated cells. a. ROS production in pimozide-treated cells. Cells were treated without (red) or with 5 μM (yellow) or 10 μM (blue) pimozide for 24 h. ROS levels were quantified using CellROX staining and flow cytometry. Representative images from one of three experiments are shown (top panels). Analysis of ROS production intensity (bottom panels). b. Cells were pretreated with NAC at the indicated concentrations for 2 h. After pretreatment, pimozide was added at the indicated concentrations and time intervals. Cells were stained with APO2.7 and analyzed using flow cytometry. Data are presented as the mean ± SD from triplicate cultures. *P < 0.001 compared to group treated only with pimozide. c. Expression of apoptosis-related proteins in pimozide-treated MT-2 cells. Cells were treated with pimozide at the indicated concentrations for 24 h and subjected to immunoblotting analysis. Actin was used as a loading control.

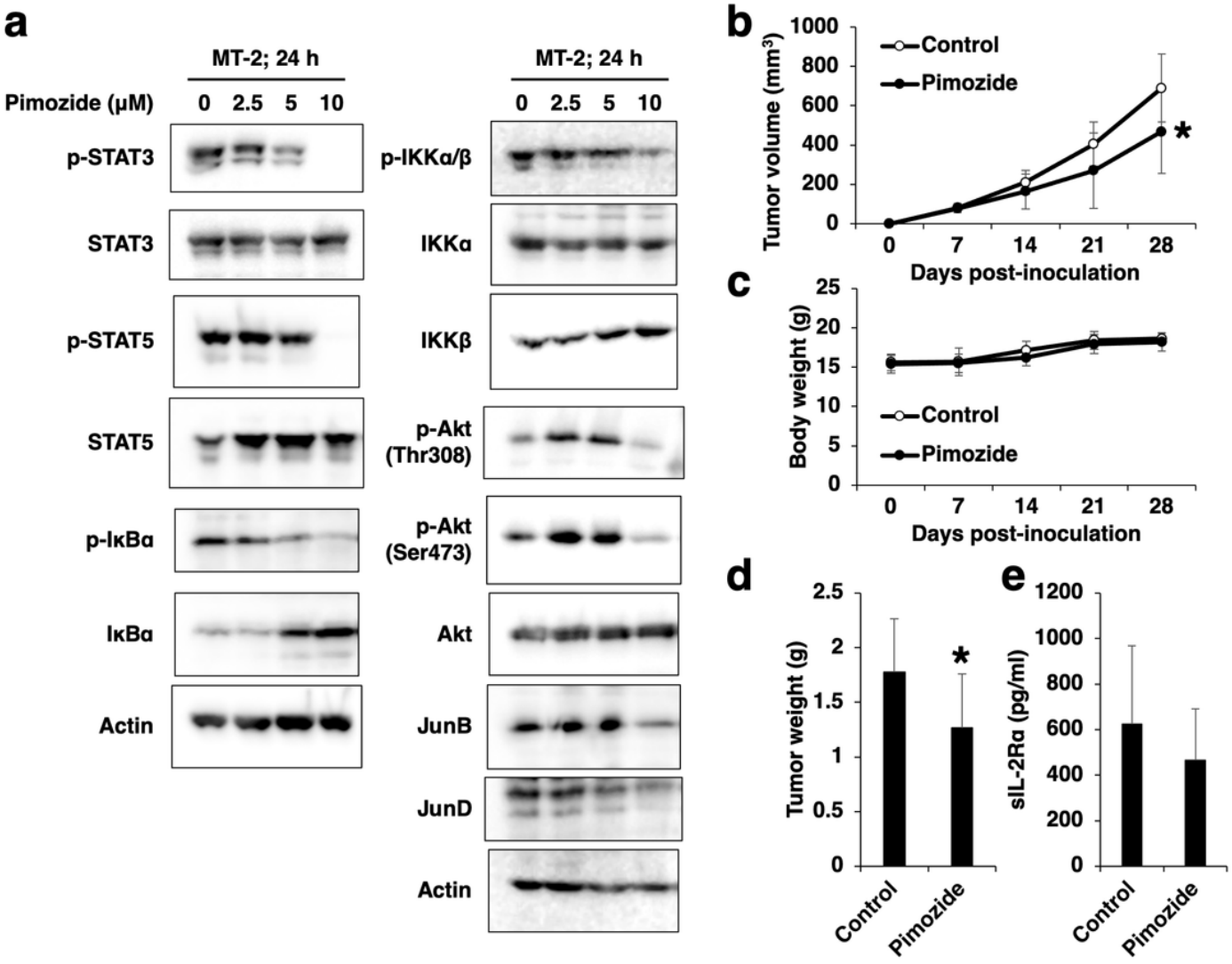

Figure 6

Pimozide affected STAT3/5, NF-κB, Akt and AP-1 activation and suppressed tumor growth in the murine xenograft model. a. Pimozide affected STAT3/5, NF-κB, Akt and AP-1 activation. MT-2 cells were treated with pimozide at the indicated concentrations for 24 h. Cell extracts were prepared to evaluate STAT3/5, NF-kB, Akt and AP-1 activation using western blot analysis. Actin was used as a loading control. b. Effect of pimozide on tumor growth in severe combined immunodeficient mice. The xenograft mice were treated with or without pimozide. Tumor size was measured weekly to calculate the tumor volume. c. Changes in the body weight of mice during the experimental period. Tumor weight (d) and serum concentrations of sIL-2Rα (e) in mice. Data are presented as the mean ± SD (n = 9). *P < 0.05 compared to controls.